TITLE

Aged male and female *Panx3* KO mice develop severe osteoarthritis independent of forced mechanical use.

Authors: Brent Wakefield[1,2], Jeffrey L. Hutchinson[2,3], Rehanna Kanji[1], Geneva Herold[3], Justin Tang[1,2], Brooke L. O'Donnell[1], Courtney Brooks[3], Patti Kiser[4], Matthew W. Grol[2,3], Cheryle A. Séguin[2,3], Silvia Penuela[1,2*], Frank Beier[2,3*].

Affiliations

[1]Department of Anatomy and Cell Biology, Schulich School of Medicine and Dentistry, University of Western Ontario, London, Ontario, N6A 5C1, Canada

[2]Western's Bone and Joint Institute, The Dr. Sandy Kirkley Centre for Musculoskeletal Research, University Hospital, London, Ontario, N6G 2V4, Canada

[3]Department of Physiology and Pharmacology, University of Western Ontario, London, Ontario, N6A 5C1, Canada

Department of Pathology and Laboratory Medicine, University of Western Ontario, London, Ontario, N6A 5C1, Canada

*To whom correspondence should be addressed:

Silvia Penuela, Ph.D., Associate Professor, Department of Anatomy and Cell Biology, University of Western Ontario, London, Ontario, Canada. Tel. 519-661-2111 ext. 84735; E-mail: spenuela@uwo.ca

Frank Beier, Ph.D., Professor and Chair, Department of Physiology and Pharmacology, University of Western Ontario, London, Ontario, N6A 5C1, Canada. Tel. 519-661-2111, ext. 85344; Email: fbeier@uwo.ca

ABSTRACT

Background: Osteoarthritis (OA) is a multi-factorial disease that is strongly associated with aging. As the molecular mechanisms underpinning the pathogenesis of this disease are partially unclear, there are no disease-modifying drugs to combat OA. The mechanosensitive channel Pannexin 3 (PANX3) has been shown to promote cartilage loss during posttraumatic OA. In contrast, the ablation of *Panx3* in male mice results in spontaneous full-thickness cartilage lesions at 24 months of age. Additionally, while protected from traumatic intervertebral disc (IVD) degeneration, *Panx3* knockout (KO) mice show signs of IVD disease with altered disc mechanics. Whether the deleterious effects of ablating *Panx3* in aging is the result from accumulated mechanical damage is unknown.

Methods: Male and female wildtype (WT) and global *Panx3* KO C57Bl6 mice were aged to 18 months of age. Mice were then randomized to sedentary (SED) or forced treadmill running (FEX) for 6 weeks (N = 5-14). Knee joint tissues including patellar tendon, quadriceps and distal patellar enthesis, and synovium were analyzed histologically, along with lumbar spine IVDs.

Results: Approximately half of male and female *Panx3* KO mice developed full-thickness cartilage lesions, severe synovitis, and ectopic fibrocartilage deposition and calcification of the knee joints. Additionally, *Panx3* KO mice with severe OA show signs of quadriceps and patellar enthesitis, characterized by bone and marrow formation. Forced treadmill running did not seem to exacerbate these phenotypes in male or female *Panx3* KO mice; however, it may have contributed to the development of lateral compartment OA. The IVDs of aged *Panx3* KO mice displayed no apparent differences to control mice, and forced treadmill running had no overt effects in either genotype.

Conclusion: Aged *Panx3* KO mice show histological features of late-stage primary OA including full-thickness cartilage erosion, subchondral bone thickening, and severe synovitis. This data suggests the deletion of *Panx3* is deleterious to synovial joint health in aging.

Introduction

Globally, knee osteoarthritis (OA) affects millions—23% of the population over 40—causing disability that results in enormous personal and socioeconomic burden [1]. While several risk

factors exist for developing OA including sex, obesity, previous joint injury, joint shape and alignment, aging is the single greatest risk factor [2]. The molecular mechanisms that underpin this age-associated destruction of synovial joints are poorly understood.

Pannexin 3 (PANX3) is a channel-forming glycoprotein expressed in osteoblasts where it can act as a Ca^{2+} release channel at the endoplasmic reticulum [3] and in chondrocytes where it can act as an ATP release channel at the cell membrane [4]. PANX3 is also expressed in annulus fibrosus (AF) cells of the intervertebral disc (IVD) [5, 6]. In an early rat model of traumatic OA (anterior crucial ligament transection), *Panx3* mRNA expression was upregulated in OA cartilage compared to control knees [7]. Additionally, in a 30-week-old mouse model, PANX3 was upregulated in cartilage following destabilization of the medial meniscus (DMM) surgery to induce post-traumatic OA [8]. This increased expression of PANX3 in diseased cartilage suggests its mechanistic involvement in traumatic OA development in rodent models. In fact, Moon *et al.* performed the DMM surgery on global and chondrocyte specific *Panx3* knockout (KO) mice and found that these mice were strongly protected from OA compared to wildtype (WT) mice [8]. Similarly, in an IVD injury model, *Panx3* KO mice had fewer hypertrophic cells of the AF, and the AF structure was largely preserved compared to WT mice [6]. These two models suggest that the absence of PANX3 is protective in traumatic/injury-induced joint disease. In humans, PANX3 is upregulated in OA cartilage tissue [8], and noncoding intronic single nucleotide polymorphisms (SNPs) of *PANX3* are strongly associated with chronic low back pain [9]. These data suggest that PANX3 function in cartilage is conserved across rodents and humans, and may be an important molecular player of OA.

Previous studies have shown that aging influences the genetic response of joint tissues to stress/injury [10-12], and therefore, aged models are required to better understand the specific mechanism of age-associated OA. To this point, male *Panx3* KO mice at 18 or 24 months of age showed accelerated cartilage erosion, subchondral sclerosis, and synovitis of the knee joint [13], which was in contrast to the previously seen protective effects in the DMM model in adult mice [8]. An important difference between the two studies is that the aged mice were given a running wheel in their cage for environmental enrichment, which could have contributed to the different effects of *Panx3* KO on joint tissues. In the IVD, we have shown that uninjured IVDs are

sensitive to aberrant biomechanical loading [6], again highlighting the context-dependent function of PANX3 in joint health.

In this study, we investigated how aging and mechanical use, via forced treadmill running, influence joint pathology in *Panx3* KO mice. *Panx3* KO mice demonstrated a bimodal distribution in which roughly half of the animals, regardless of forced running, had full-thickness cartilage erosion down to the subchondral bone and expanded synovium containing ectopic calcification and fibrocartilage with scattered lymphocytes, while the other half had mild synovitis. In contrast, WT mice had mild signs of superficial cartilage erosion and synovitis. Male *Panx3* KO mice also displayed cartilage, bone, and bone marrow in the quadriceps enthesis reminiscent of enthesitis. The degree to which these mice had enthesitis or tendinopathy of the knee was correlated with OA scores. At the lumbar spine, *Panx3* KO mice IVDs were histologically similar to WT mice. These results suggest that aged *Panx3* KO mice, regardless of sex and activity, develop severe knee joint pathology including OA in aging.

Methods

Mice

Animals used in this study were bred in-house and euthanized in accordance with the ethics guidelines of the Canadian Council for Animal Care. Animal use protocols were approved by the Council for Animal Care at Western University Canada (AUP 2019-069). Mice were housed in standard shoe box-style caging, and exposed to a 12-hour light/dark cycle and ate regular chow *ad libitum*. WT and *Panx3* KO mice were congenic [8]. DNA was collected from ear clippings of each mouse to determine the genotype using polymerase chain reaction (PCR) as previously described [8, 14]. At sacrifice, mouse knees and spines were collected and immediately processed for histological analysis.

Forced treadmill running

At 18 months, mice were randomized to either a no exercise group (sedentary, SED) or a forced treadmill running (forced-exercise, FEX) group. FEX groups ran on a treadmill (Columbus Instruments, Ohio) for 6 weeks, 1 hour a day for 5 days a week, at a speed of 11 m/min, and a 10° incline—an adapted protocol that has previously been used to induce OA in male C57BL/6

mice [15]. Per the animal ethics protocol, the mice were encouraged to run using a bottle brush bristle and a shock grid at the end of the treadmill.

Histopathological assessment of the knee joint

At the experimental endpoint, knee joints were fixed in 4% paraformaldehyde at room temperature for 24 hours on a shaker and then decalcified in 5% EDTA for 12 days at room temperature. Knees were processed and embedded in the sagittal plane in paraffin, and 6-µm–thick sections were cut from front to back. Sections were stained with toluidine blue. Three sections from the medial and lateral compartments were scored by 2 blinded reviewers using the Osteoarthritis Research Society International (OARSI) recommendations for histological assessments of OA in the mouse [16]. The average max score of each sample was then used for statistical analysis.

Synovial tissue pathological assessment

Considering the severity and bimodal distribution of the phenotype in these animals, we opted to take a more descriptive approach when describing the synovial changes that were occurring within these animals versus a semi-quantitative analysis. A pathologist with experience describing joint disease in animal models investigated the occurrence of specific pathological features observed in the synovium of the animals. The pathologist was blinded to all genotypes, sex, and activity. One hematoxylin and eosin (H&E)-stained section of the medial load-bearing region per animal was selected for analysis.

Enthesis and patellar tendon analysis

Mid-tendon sections were stained with toluidine blue and scored for distal quadriceps tendon enthesitis, distal patellar tendon enthesitis and patellar tendinopathy. Enthesitis was scored using the following parameters: 0 = normal; 1 = ectopic cartilage; 2 = ectopic cartilage/bone; 3 = ectopic cartilage/bone with a marrow cavity; 4 = ectopic bone with a marrow. Tendinopathy was scored using the following system: 0 = normal; 1 = increased cellularity; 2 = cell rounding/clustering; 3 = chondrogenesis (i.e., proteoglycan-rich matrix, hypertrophy); 4 = ectopic cartilage/bone.

Histopathological assessment of the lumbar intervertebral discs

Lumbar spines were fixed for 24 hours with 4% paraformaldehyde, followed by 7 days of decalcification with Shandon's TBD-2 (Thermo Fisher Scientific, Waltham, MA, USA) at room temperature. Tissues were embedded in paraffin and sectioned in the sagittal plane at a thickness of 5 µm. Mid-sagittal sections were deparaffinized and rehydrated as previously described [17] and stained using 0.1% Safranin-O/0.05% Fast Green. Sections were imaged on a Leica DM1000 microscope, with Leica Application Suite (Leica Microsystems: Wetzlar, DEU). To evaluate IVD degeneration, spine sections were scored by two observers blinded to age, exercise, sex, and genotype using a previously established histopathological scoring system for mouse IVDs [18]. Alterations to the scoring system were made, in which we excluded a score of 4 for the NP: "mineralized matrix in the NP". To report on degeneration across the lumbar spine, scores for individual lumbar IVDs (L2-L6) were averaged, and the total score plotted for each individual mouse.

Statistics

The Department of Epidemiology and Biostatistics at Western University was consulted to determine the appropriate statistical analysis. Data are presented as stated in the respective figure. Prism 9 (GraphPad Software Inc.) Version 9.4.1 (458) was used to run all statistical tests including one-way analysis of variance (ANOVA) or two-way ANOVA for comparison. For OARSI scores, histopathological scores of the IVD, enthesitis and tendinopathy scores, males and females were analyzed separately within their respective genotypes and activity group. A Kruskal-Wallis test was used with an uncorrected Dunn's test for multiple comparisons to determine statistical differences among the groups. Correlations were performed using Pearson's r. All applicable data met assumptions for homoscedasticity or normality of residuals. Based on the recommendations of the editorial entitled: Moving to a World Beyond "$p < 0.05$" [19] we did not set a threshold for significance, and data is referred to in terms of weak, moderate or strong statistical evidence.

Results

Panx3 KO mice have comparable body weights to WT mice under sedentary and forced treadmill running conditions within their respective sex.

Since we have previously published large reductions in body weights of *Panx3* KO mice compared to WT mice in adulthood [20], we first investigated the effect of deleting *Panx3* on body weight in aged animals (Figure 1) and found that those genotypic differences were diminished with age. There was weak statistical evidence for differences in body weight between genotypes in both male (Figure 1A) and female (Figure 1B) mice. While there was weak statistical evidence for body weight differences between activity groups in males, there was moderate statistical evidence for female mice to have lower body weights when forced to run on a treadmill for 6 weeks compared to SED female mice. This data suggests aged WT and *Panx3* KO mice have similar body weights under SED and FEX conditions.

Male Panx3 KO mice develop full-thickness cartilage erosion of the tibia and femur surface in aging.

Next, we assessed whether male *Panx3* KO mice develop histopathological OA compared to WT mice in aging, and whether forced treadmill running would influence these outcomes. Toluidine blue-stained, paraffin-embedded sections from the knee joints of 18-month-old WT and *Panx3* KO mice under SED or FEX conditions were analyzed. Histologically, full-thickness cartilage lesions were observed in half of the *Panx3* KO mice in the medial tibial and femoral surfaces but not in any of the WT mice (Figure 2A, B, D). Additionally, this subset of *Panx3* KO mice displayed thickening of the subchondral bone plate (Figure 2A). In the lateral compartment, there was weak statistical evidence for differences between SED WT and SED *Panx3* KO mice (Figure 2A, D, E). Regarding the effect of forced treadmill running, there was weak statistical evidence that the addition of forced treadmill running influenced the cartilage structure in both knee compartments of WT mice. In the lateral compartment, there was moderate statistical evidence that FEX *Panx3* KO mice had worse OARSI scores compared to SED WT mice, as 3 mice had full-thickness lesions of the tibia (Figure 2C); however, there was weak statistical evidence for differences in femur OARSI scores among the groups (Figure 2E). Taken together, this suggests male *Panx3* KO mice develop histological features of severe OA in the medial

compartment, while the combination of *Panx3* deletion and forced treadmill running results in lateral compartment erosion.

Female Panx3 KO mice develop full-thickness cartilage erosion of the tibia and femur medial compartment in aging.

Next, we performed the same histological analysis of female knees from aged WT and *Panx3* KO mice under SED and FEX conditions. Note, female mice had not been included in our earlier aging study [21]. Like in males, several female *Panx3* KO mice developed full-thickness cartilage erosion in the medial compartment (6 mice in total), along with thickening of the subchondral bone, while no WT mice developed such erosion (Figure 3A, B, C). Forced treadmill running seemed to have little to no effect on cartilage structure in the medial compartment (Figure 3A, B, C). In the lateral compartment, while some SED *Panx*3 KO mice showed signs of cartilage erosion, full thickness erosion was only observed in some *Panx3* KO mice (N = 3) that were forced to run, but there was weak statistical inference to suggest differences between these groups (Figure 3D, E). This data suggests, like male *Panx3* KO mice, female mice exhibit a bimodal distribution, with a subset of mice developing full-thickness cartilage erosion, and the addition of forced treadmill running may influence development of cartilage loss of the tibia in the lateral compartment.

Panx3 KO mice develop mild to severe synovitis under both sedentary and forced treadmill running conditions.

Considering the bimodal distribution seen in our KO mice, and upon observation of the severe synovial changes in the mice with full-thickness erosions, we chose to take a descriptive approach for the synovial analysis. Synovial tissue was assessed by a blinded pathologist with extensive experience describing animal model synovial tissue. H&E-stained sections in the medial load-bearing zone were assessed. Three distinct joint morphological phenotypes were observed across the groups: 1) no lesions (Figure 4A); 2) mild acute synovitis (Figure 4B); 3) and severe diffuse synovial fibrosis with ectopic ossification (Figure 4C). All samples with mild to severe synovitis were from *Panx3* KO mice, except for one WT sample. Synovium of *Panx3*

KO mice with intact cartilage consisted of acute lymphocytic synovitis, where the synovium was expanded by lymphocytes and few macrophages (Figure 4B mild synovitis). Full-thickness cartilage erosion in the *Panx3* KO mice coincided with severe diffuse synovial fibrosis, ulceration, and ectopic ossification (Figure 4C severe synovitis). These mice had locally extensive to complete effacement of the synovium by collagen, fibrocartilage and in some cases, bone interrupted by areas of acellular basophilic material. These findings suggest that aged *Panx3* KO mice develop mild-to-severe synovitis of the knee joint, which coincides with the severity of cartilage erosion.

Male Panx3 KO mice display ectopic cartilage and bone deposits containing marrow in the enthesis of the quadriceps and patellar tendons.

Considering the enthesis originates from fibrocartilage cells that are highly responsive to mechanical loading [22], we next analyzed the patellar tendon for signs of tendinopathy and enthesitis at the distal patella and quadriceps tendons (Figures 5&6A). In male mice, there was moderate statistical evidence suggesting SED *Panx3* KO mice develop enthesitis of the quadriceps tendon enthesis, consisting of cartilage and bone deposits, often with a marrow cavity (Figure 5B). Throughout the patellar tendon, there was weak statistical evidence for histopathological cellular changes in any of the groups (Figure 5C). Like the quadriceps enthesis, the distal patellar tendon enthesis of SED *Panx3* KO mice showed signs of enthesitis, including deposits of cartilage and bone, often with a marrow cavity, compared to SED WT mice (Figure 5D). In female mice, we performed the same semi-quantitative analysis of the enthesis and patellar tendon (Figure 6A). At the quadriceps enthesis, there was moderate statistical evidence that *Panx3* KO mice develop enthesitis with forced treadmill running (Figure 6B), with all the mice showing ectopic cartilage and bone, often with marrow formation, within the quadriceps tendon enthesis (Figure 6E). Throughout the patellar tendon, there was weak statistical evidence for histopathological changes to cellular shape or distribution among the groups (Figure 6C). At the patellar tendon enthesis, there was moderate statistical evidence that WT mice develop enthesitis with forced treadmill running, with weak statistical evidence of histological differences in *Panx3* KO mice (Figure 6D). This data suggests that *Panx3* KO mice develop enthesitis of the quadriceps and patellar tendon entheses during aging, while forced treadmill running in female WT mice produced enthesitis at the distal patellar tendon enthesis. We next ran a Pearson's

correlation between medial OA scores and the enthesitis and tendinopathy scores to determine if there was a relationship between which mice develop OA and those that develop enthesis and tendon pathology. There was strong statistical evidence suggesting that higher enthesitis and tendinopathy scores coincided with higher OA scores (Table 1).

Table 1: Medial tibial OARSI scores correlate with tendinopathy and enthesitis scores.

	OARSI Score	Tendinopathy	Quadriceps Enthesitis	Patellar Enthesitis
OARSI Score	-			
Tendinopathy	0.38 $p = 0.001$	-		
Quadriceps Enthesitis	0.38 $p = 0.002$	0.27 $p = 0.029$	-	
Patellar Enthesitis	0.58 $p < 0.001$	0.32 $p = 0.008$	0.19 $p = 0.127$	-

Panx3 KO mouse IVDs age normally in males and females even when forced to treadmill run. To investigate the role of PANX3 in age-associated IVD degeneration, and whether forced treadmill running in aging influences disc health, we next analyzed the IVDs for histological changes. WT and *Panx3* KO mice were aged to 18 months and lumbar spines were analyzed histologically as described in the Methods section. Under both SED and FEX conditions, male (Figure 7A, B) and female (Figure 7C, D) *Panx3* KO IVDs appeared normal relative to WT controls with no differences in histopathological features of degeneration in the nucleus pulposus (NP) and the AF at any disc height (Figure 7A, C) or when averaged across the lumbar spine (Figure 7B, D). This data suggests that the IVDs of both male and female *Panx3* KO mice, age and respond to forced treadmill running similarly to their WT counterparts.

Discussion

In this study, we found that 18-month-old male and female *Panx3* KO mice demonstrate severe OA of the knee, while their IVDs seem to be histologically comparable to the WT mouse

controls. The addition of forced mechanical loading through treadmill running does not exacerbate this phenotype in the medial compartment, while a subset of FEX *Panx3* KO mice had full-thickness lesions in the lateral compartment, suggesting a compartment-specific effect of forced treadmill running in *Panx3* KO mice. Additionally, *Panx3* KO mice develop mild to severe synovitis consisting of lymphocyte infiltration, and ectopic fibrocartilage and calcification of the knee joint. Male *Panx3* KO mice also appeared to have histological features of quadriceps and patellar tendon enthesitis under SED conditions, whereas female *Panx3* KO mice developed quadriceps enthesitis tendon with forced treadmill running. Within lumbar spine IVDs, both male and female *Panx3* KO mice had similar histopathological features to the WT controls. Even with the stress of forced treadmill running, there was weak statistical evidence for histopathological differences among the groups, suggesting running later in life is not detrimental to disc structure in either genotype.

Full-thickness cartilage erosion is not a normal histological feature of knee joints in aged mice [23]. In this study, the full-thickness cartilage loss observed in our animals was accompanied by erosion and fibrillation of adjacent cartilage surfaces. However, it was not apparent based on remaining tissue, whether the ulceration was an artifact (i.e., loss of resident degenerate cartilage during processing) or a true pre-mortem condition. We think the former is more likely, based on the lack of surface remodeling of this exposed bone to suggest chronic injury. It is possible, however, that a delay in bone remodelling is a feature of *Panx3* KO mice, which could be possible considering their known function as promoter of osteoblast differentiation [24, 25]. This is not to suggest that the cartilage of these *Panx3* KO mice is not degenerating, but rather histological representation may not accurately depict the *in vivo* state of the cartilage tissue pre-mortem. Using μ-CT contrast imaging of cartilage will allow for the determination of whether these mice have true full-thickness cartilage lesions – a goal of future studies.

In addition to cartilage erosion, we saw mild to severe synovitis in the *Panx3* KO animal knees, which included extensive fibrocartilage and calcification deposition within the synovium. Whether PANX3 is expressed in synovial tissue has not been determined; however, *in silico* data suggests *PANX3* should be expressed in human synovial fibroblasts [26]. Additionally, considering the severe inflammatory phenotype, we are unaware of any indication that

macrophages or lymphocytes express *Panx3.* Future studies should investigate the periarticular expression and function of *Panx3* in joint tissues.

Considering the evidence showing PANX3's role in cartilage, it is possible that the synovial phenotype is initiated by cartilage degradation and subsequent synovitis. Chronic release of damage-associated molecular patterns or other catabolic signals (e.g. cytokines) from degrading cartilage into the synovial fluid space may activate synovial lining macrophages [27]. In our previous report challenging 30-week-old *Panx3* KO mice, we showed superficial cartilage erosion which was exacerbated by forced treadmill running and resulted in moderate evidence of synovial lining thickening, suggesting early OA development (under review). A lifetime of cartilage erosion may be chronically stimulating synovial macrophages leading to these pathological changes. Previously, we found that aged *Panx3* KO mice had low lubricin expression in the superficial zone of the articular cartilage [13]. Lubricin is an essential lubricating protein for the joint surface [28], and *in vitro* models have shown that lubricin has anti-inflammatory effects on synovial lining fibroblasts by binding to toll-like receptors 2 and 4 [29]. Taken together, the superficial erosion in adulthood of *Panx3* KO mice may lead to reduced lubricin levels in aging, which could be chronically activating synovial lining cells, and thus producing the severity of synovitis we observed in the present study.

Inflammation is associated with age-related pathologies [30] including primary OA, and nuclear Factor Kappa β (NF-κβ) is a proposed central pathway of inflammation in OA [23]. Interestingly, through mechanotransduction pathways, chondrocytes can release ATP, and this extracellular ATP has been shown to activate NF-κβ signalling and contribute to OA [31, 32]. While some ATP release is required to maintain normal cartilage homeostasis [33], abnormal mechanical loading of cartilage increases chondrocyte ATP release [34, 35]. This suggests that there are physiologically healthy levels of ATP release required for cartilage maintenance, but dysregulation of this mechanism could contribute to inflammation and OA. Our previous reports showed that aging WT mouse cartilage maintains similar PANX3 protein expression at 6, 18, and 24 months of age [13], suggesting PANX3 is required to maintain cartilage health well into aging. Deletion of *Panx3* may dysregulate this ATP signalling given its canonical function as a mechanosensitive, plasma membrane ATP release channel in cells such as chondrocytes [4, 36].

In our previous report, *Panx3* deletion did not significantly impact the progression of age-associated histopathological IVD degeneration in male mice at 18 and 24 months of age compared to WT mice [6]. The present study also determined that the aged female *Panx3* KO mice IVD histopathological analysis matched that of males. The contrasting difference between the knee joint and IVDs of *Panx3* KO mice is interesting considering the similar mechanism of disease progression between OA and IVD diseases [37]. It appears that PANX3 is not essential to IVD health during normal aging, as our previous report showed low transcript expression of *Panx3* in IVDs from 6 to 24 months of age relative to levels at 2 months of age [6]. It is possible that PANX3 is utilized in early life and development of the IVD, while dispensable in aging. Interestingly, forced treadmill running seemed to have no effect on histological features of the IVDs regardless of genotype or sex. This was surprising, considering *Panx3* KO mice developed histopathological features in the AF of IDD with forced treadmill running in adult mice (under review). It was reasonable to hypothesize that aging would have rendered these mice more susceptible to forced treadmill running-induced changes to the IVD. However, considering aging alone results in relatively severe spontaneous IDD in mice [38], any potential impact of forced treadmill running, positive or negative, may have been undetectable with histopathological scoring.

Future studies should involve a time course of *Panx3* KO mouse OA development. Specifically, analyzing earlier time points (for example. 6, 9, and 12 months) to determine when distinct OA phenotypes arise, and to characterize its progression. This will allow for the analysis of the early cellular changes that may be driving this severe OA. Additionally, considering that obesity is a strong risk factor for OA, and coincides with aging, high-fat diet studies in *Panx3* KO mice are also warranted. Lastly, tissue-specific KO models using various Cre driver lines are also warranted to determine the cell type responsible for this severe OA development.

Conclusion

Aged male and female *Panx3* KO mice develop severe OA under both SED and FEX conditions, and that this occurs spontaneously as in human primary OA. Additionally, *Panx3* KO mice have enthesitis of the quadriceps and distal patella more often than WT mice, but at the lumbar IVDs, *Panx3* KO mice have similar histological features as WT mice in aging. Collectively, our data

suggests chronic suppression of PANX3 throughout life may be contraindicated and cause severe OA. Potential therapeutic interventions could include agonists of PANX3 to overcome the lower expression or reduced functionality of PANX3 channels in aged joint tissues.

References

1. Cui, A., et al., *Global, regional prevalence, incidence and risk factors of knee osteoarthritis in population-based studies.* EClinicalMedicine, 2020. **29-30**: p. 100587.
2. Johnson, V.L. and D.J. Hunter, *The epidemiology of osteoarthritis.* Best Pract Res Clin Rheumatol, 2014. **28**(1): p. 5-15.
3. Bond, S.R., et al., *Pannexin 3 is a novel target for Runx2, expressed by osteoblasts and mature growth plate chondrocytes.* J Bone Miner Res, 2011. **26**(12): p. 2911-22.
4. Iwamoto, T., et al., *Pannexin 3 regulates intracellular ATP/cAMP levels and promotes chondrocyte differentiation.* J Biol Chem, 2010. **285**(24): p. 18948-58.
5. Veras, M.A., et al., *Transcriptional profiling of the murine intervertebral disc and age-associated changes in the nucleus pulposus.* Connect Tissue Res, 2020. **61**(1): p. 63-81.
6. Serjeant, M., et al., *The role of Panx3 in age-associated and injury-induced intervertebral disc degeneration.* Int J Mol Sci, 2021. **22**(3): p. 1-15.
7. Appleton, C.T., et al., *Global analyses of gene expression in early experimental osteoarthritis.* Arthritis Rheum, 2007. **56**(6): p. 1854-68.
8. Moon, P.M., et al., *Deletion of Panx3 prevents the development of surgically induced osteoarthritis.* J Mol Med (Berl), 2015. **93**(8): p. 845-56.
9. Belonogova, N.M., et al., *Noncoding rare variants in PANX3 are associated with chronic back pain.* Pain, 2023. **164**(4): p. 864-869.
10. Sebastian, A., et al., *Global Gene Expression Analysis Identifies Age-Related Differences in Knee Joint Transcriptome during the Development of Post-Traumatic Osteoarthritis in Mice.* Int J Mol Sci, 2020. **21**(1).
11. Loeser, R.F., et al., *Microarray analysis reveals age-related differences in gene expression during the development of osteoarthritis in mice.* Arthritis Rheum, 2012. **64**(3): p. 705-17.
12. Iijima, H., et al., *Meta-analysis Integrated With Multi-omics Data Analysis to Elucidate Pathogenic Mechanisms of Age-Related Knee Osteoarthritis in Mice.* J Gerontol A Biol Sci Med Sci, 2022. **77**(7): p. 1321-1334.
13. Moon, P.M., et al., *Global deletion of pannexin 3 resulting in accelerated development of aging-induced osteoarthritis in mice.* Arthritis Rheum, 2021. **73**(7): p. 1178-1188.
14. Abitbol, J.M., et al., *Double deletion of Panx1 and Panx3 affects skin and bone but not hearing.* J Mol Med (Berl), 2019. **97**(5): p. 723-736.
15. Bomer, N., et al., *The effect of forced exercise on knee joints in Dio2(-/-) mice: type II iodothyronine deiodinase-deficient mice are less prone to develop OA-like cartilage damage upon excessive mechanical stress.* Ann Rheum Dis, 2016. **75**(3): p. 571-7.
16. Glasson, S.S., et al., *The OARSI histopathology initiative - recommendations for histological assessments of osteoarthritis in the mouse.* Osteoarthr. Cartil., 2010. **18 Suppl 3**: p. 17-23.
17. McCann, M.R., et al., *Repeated exposure to high-frequency low-amplitude vibration induces degeneration of murine intervertebral discs and knee joints.* Arthritis Rheumatol, 2015. **67**(8): p. 2164-75.
18. Tam, V., et al., *Histological and reference system for the analysis of mouse intervertebral disc.* J Orthop Res, 2018. **36**(1): p. 233-243.
19. Wasserstein, R.L., A.L. Schirm, and N.A. Lazar, *Moving to a world beyond "p < 0.05".* American Statistician, 2019. **73**: p. 1-19.
20. Wakefield, C.B., et al., *Pannexin 3 deletion reduces fat accumulation and inflammation in a sex-specific manner.* Int J Obes (Lond), 2022. **46**(4): p. 726-738.

21. Moon, P.M., et al., *Global Deletion of Pannexin 3 Accelerates Development of Aging-induced Osteoarthritis in Mice.* Arthritis Rheumatol, 2021: p. 1178-1188.
22. Schwartz, A.G., F. Long, and S. Thomopoulos, *Enthesis fibrocartilage cells originate from a population of Hedgehog-responsive cells modulated by the loading environment.* Development, 2015. **142**(1): p. 196-206.
23. Catheline, S.E., et al., *IKKβ-NF-κB signaling in adult chondrocytes promotes the onset of age-related osteoarthritis in mice.* Sci. Signal., 2021. **14**(701): p. 1-39.
24. Ishikawa, M., et al., *Pannexin 3 functions as an ER Ca(2+) channel, hemichannel, and gap junction to promote osteoblast differentiation.* J Cell Biol, 2011. **193**(7): p. 1257-74.
25. Ishikawa, M., et al., *Pannexin 3 ER Ca(2+) channel gating is regulated by phosphorylation at the Serine 68 residue in osteoblast differentiation.* Sci Rep, 2019. **9**(1): p. 1-14.
26. Baranova, A., et al., *The mammalian pannexin family is homologous to the invertebrate innexin gap junction proteins.* Genomics, 2004. **83**(4): p. 706-16.
27. Millerand, M., F. Berenbaum, and C. Jacques, *Danger signals and inflammaging in osteoarthritis.* Clin Exp Rheumatol, 2019. **37 Suppl 120**(5): p. 48-56.
28. Rhee, D.K., et al., *The secreted glycoprotein lubricin protects cartilage surfaces and inhibits synovial cell overgrowth.* J Clin Invest, 2005. **115**(3): p. 622-31.
29. Iqbal, S.M., et al., *Lubricin/Proteoglycan 4 binds to and regulates the activity of toll-like receptors in vitro.* Sci. Rep., 2016. **6**(1): p. 1-12.
30. Josephson, A.M., et al., *Age-related inflammation triggers skeletal stem/progenitor cell dysfunction.* Proc Natl Acad Sci U S A, 2019. **116**(14): p. 6995-7004.
31. Ferrari, D., et al., *Extracellular ATP activates transcription factor NF-kappaB through the P2Z purinoreceptor by selectively targeting NF-kappaB p65.* J Cell Biol, 1997. **139**(7): p. 1635-43.
32. Li, Z., et al., *P2X7 receptor induces pyroptotic inflammation and cartilage degradation in osteoarthritis via NF-κB/NLRP3 crosstalk.* Oxid Med Cell Longev, 2021. **2021**: p. 1-16.
33. Millward-Sadler, S.J., et al., *ATP in the mechanotransduction pathway of normal human chondrocytes.* Biorheology, 2004. **41**(3-4): p. 567-75.
34. Garcia, M. and M.M. Knight, *Cyclic loading opens hemichannels to release ATP as part of a chondrocyte mechanotransduction pathway.* J Orthop Res, 2010. **28**(4): p. 510-5.
35. Leong, W.S., R.G. Russell, and A.M. Caswell, *Stimulation of cartilage resorption by extracellular ATP acting at P2-purinoceptors.* Biochim Biophys Acta, 1994. **1201**(2): p. 298-304.
36. Pillon, N.J., et al., *Nucleotides released from palmitate-challenged muscle cells through pannexin-3 attract monocytes.* Diabetes, 2014. **63**(11): p. 3815-26.
37. Fine, N., et al., *Intervertebral disc degeneration and osteoarthritis: a common molecular disease spectrum.* Nat. Rev. Rheumatol., 2023. **19**(3): p. 136-152.
38. Ohnishi, T., et al., *Age-related spontaneous lumbar intervertebral disc degeneration in a mouse model.* J Orthop Res, 2018. **36**(1): p. 224-232.

Figure Legends

Figure 1: Aged *Panx3* KO mice have similar body weights to WT mice under sedentary and forced treadmill running conditions within each sex.

WT and *Panx3* KO mice were aged to 18 months of age and randomized to either sedentary (SED) or forced treadmill running (FEX) for 6 weeks. Body weights were taken at termination. WT SED (N = 9), WT FEX (N = 10), KO SED (N = 11), and KO FEX (N = 10), as indicated. Male body weights (A). Female body weights (B). WT SED (N = 12), WT FEX (N = 9), KO SED (N = 4), and KO FEX (N = 11), as indicated. For statistical comparisons among the groups, a two-way ANOVA with genotype x activity was used with a Tukey's correction for multiple comparisons. All data are shown as means ± CI.

Figure 2: Half of male *Panx3* KO mice develop full-thickness cartilage erosion of the medial tibia and femur regardless of forced treadmill running.

Representative toluidine blue staining of knee joints from male wildtype (WT) and *Panx3* knockout (KO) mice under sedentary (SED) and forced treadmill running (FEX) conditions, as indicated (A). Whole joint images were taken at 4x magnification (scale bar = 500µm) and 10x magnification of the cartilage (scale bar = 100µm) of the medial (left) and lateral (right) compartments. Double black arrows show cartilage erosion to the subchondral bone. Green arrows show superficial cartilage erosion, and red arrows show erosion to the calcified cartilage. (B – E) Violin plots showing the distribution/grouping of medial tibia (B) and femur (C) and lateral tibia (D) and femur (E) OARSI max scores of male mice for WT SED (N = 10), WT FEX (N = 10), KO SED (N = 10), and KO FEX (N = 9), as indicated. For statistical comparisons among the groups, a Kruskal-Wallis test was performed.

Figure 3: A subset of female *Panx3* KO mice develop full-thickness cartilage erosion of the medial tibia and femur regardless of forced treadmill running.

Representative toluidine blue staining of knee joints from female wildtype (WT) and *Panx3* knockout (KO) mice under sedentary (SED) and forced treadmill running (FEX) conditions, as

indicated (A). Whole joint images were taken at 4x magnification (scale bar = 500μm) and 10x magnification of the cartilage (scale bar = 100μm) at the medial (left) and lateral (right) compartments. Double black arrows show cartilage erosion to the subchondral bone. Green arrows show superficial cartilage erosion, and red arrows show erosion to the calcified cartilage. (B – E) Violin plots showing the distribution/grouping of medial tibia (B) and femur (C) and lateral tibia (D) and femur (E) OARSI max scores of female mice. WT SED (N = 12), WT FEX (N = 9), KO SED (N = 5), and KO FEX (N = 11), as indicated. For statistical comparisons among the groups, a Kruskal-Wallis test was performed.

Figure 4: *Panx3* KO mice develop mild to severe synovitis of the knee in aging.

Sagittal sections of the medial compartment were stained with H&E and assessed by a blinded pathologist. Slides were assessed for signs of immune cell infiltration of the synovial lining (black arrows), indicating mild synovitis, which was a phenotype of *Panx3* KO mice (one WT mouse was characterized to have mild synovitis). Ectopic ossification (yellow arrows) and fibrocartilage (green arrows) were observed exclusively in *Panx3* KO mice and was characterized as severe lesions. * Denotes cartilage erosion. + denoting loss of synovial lining. Whole joint images (Left) are 4x magnification. Scale bar = 500μm. Posterior synovium (middle) are 10x magnification. Scale bar = 100μm. Lining (right) images are 20x magnification. Scale bar = 100μm.

Figure 5: Sedentary male *Panx3* KO mice show signs of patellar and quadriceps enthesitis.

Male WT and *Panx3* KO knee sections were stained with toluidine blue, sectioned in the sagittal plane and scored for quadriceps enthesitis (A1), patellar tendinopathy (A2), and patellar enthesitis (A3). Sedentary (SED), and forced treadmill running (FEX). Violin plots showing distribution/grouping of histological scores for quadriceps enthesitis (B), tendinopathy (C), and patellar enthesitis (D). Representative toluidine blue sagittal sections (E). 10x magnification. Scale bar = 100 μm. Black arrows point to cartilage, yellow arrows point to bone and marrow. WT SED (N = 8), WT FEX (N = 10), KO SED (N = 12), and KO FEX (N = 11). For statistical comparisons among the groups, a Kruskal-Wallis test was performed.

Figure 6: Female *Panx3* KO mice develop quadriceps enthesitis with forced treadmill running.

Female WT and *Panx3* KO knee sections were stained with toluidine blue, sectioned in the sagittal plane and scored for quadriceps enthesitis (A1), patellar tendinopathy (A2), and patellar enthesitis (A3). Sedentary (SED), and forced treadmill running (FEX). Violin plots showing distribution/grouping of histological scores for quadriceps enthesitis (B), tendinopathy (C), and patellar enthesitis (D). Representative toluidine blue sagittal sections (E). 10x magnification. Scale bar = 100 μm. black arrows point to cartilage, yellow arrows point to bone and marrow. WT SED (N = 14), WT FEX (N = 8), KO SED (N = 4), and KO FEX (N = 11). For statistical comparisons among the groups, a Kruskal-Wallis test was performed.

Figure 7: No overt differences in histopathological scores of the IVDs between WT and *Panx3* KO mice.

Wildtype (WT) and *Panx3* KO (KO) mouse lumbar spines were stained with Safranin O Fast Green. Histopathological scores for males by disc height (A) and average disc score across the lumbar spine (B). WT SED (N = 8), WT FEX (N = 10), KO SED (N = 12), and KO FEX (N = 11). Female histopathological scores by disc height (C) and average disc score across the lumbar spine (D). WT SED (N = 14), WT FEX (N = 8), KO SED (N = 4), and KO FEX (N = 11). For statistical comparisons among the groups, a Kruskal-Wallis test was performed. All data are shown as means ± CI.

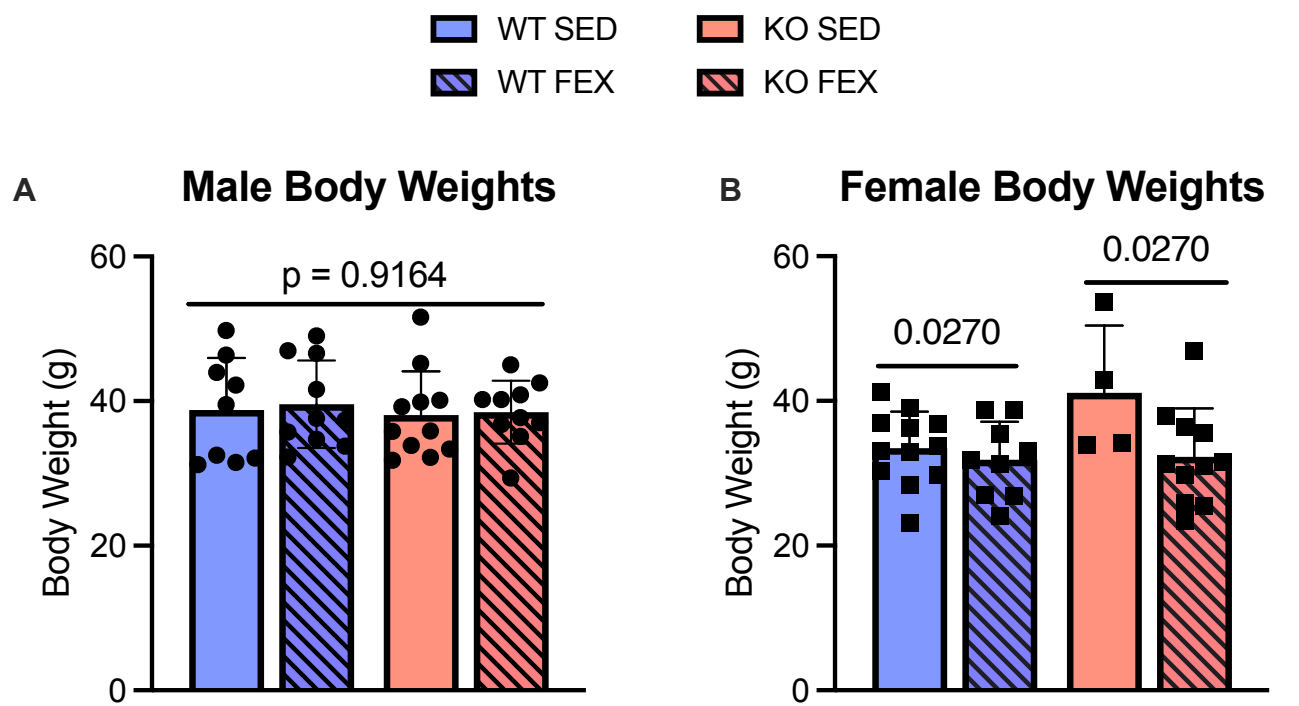
WT SED
WT FEX
KO SED
KO FEX
A
Male Body Weights
Body Weight (g)
60
40
20
0
p = 0.9164
B
Female Body Weights
Body Weight (g)
60
40
20
0
0.0270
0.0270

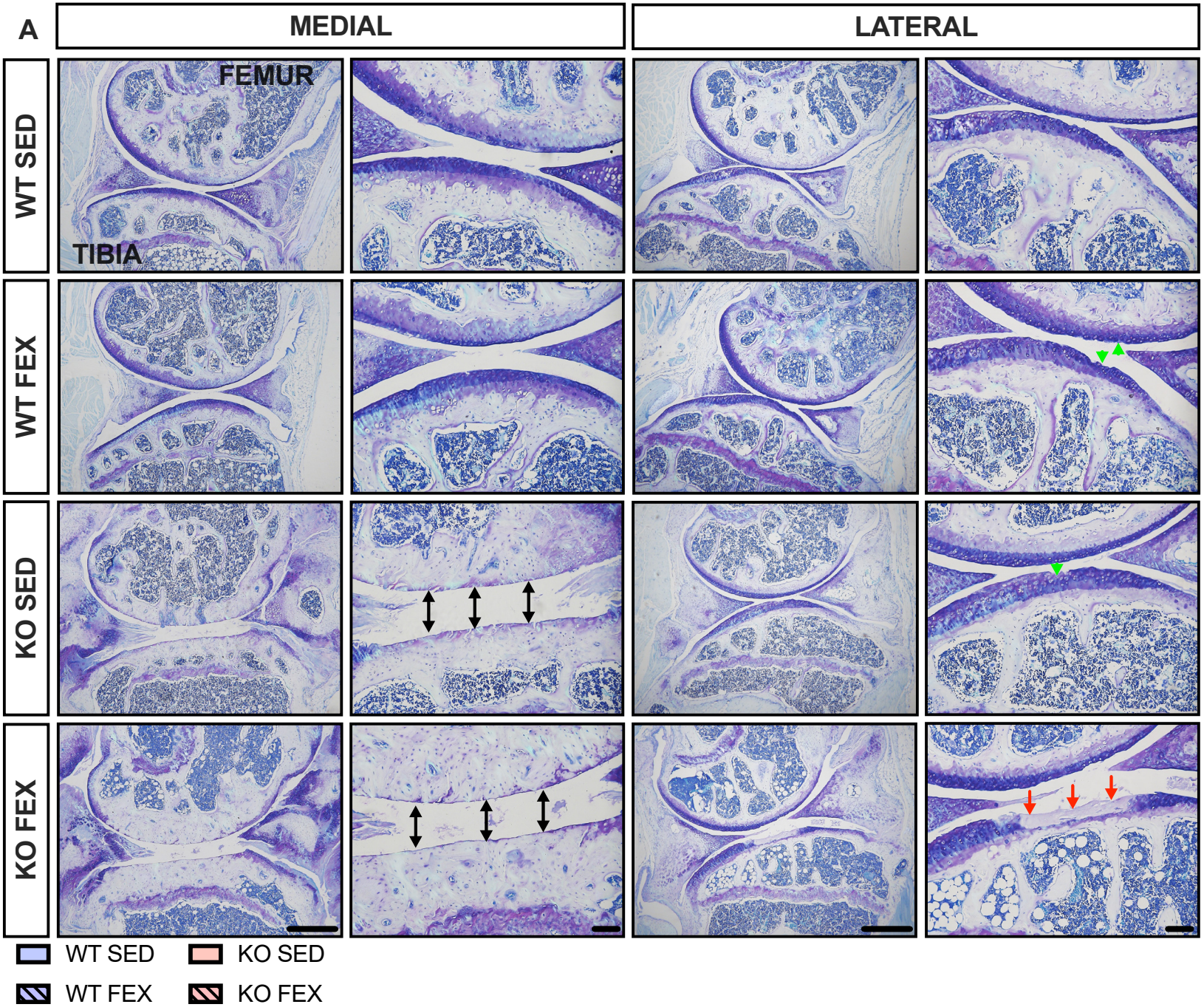
A
MEDIAL
LATERAL
WT SED
WT FEX
KO SED
KO FEX
FEMUR
TIBIA
WT SED
KO SED
WT FEX
KO FEX

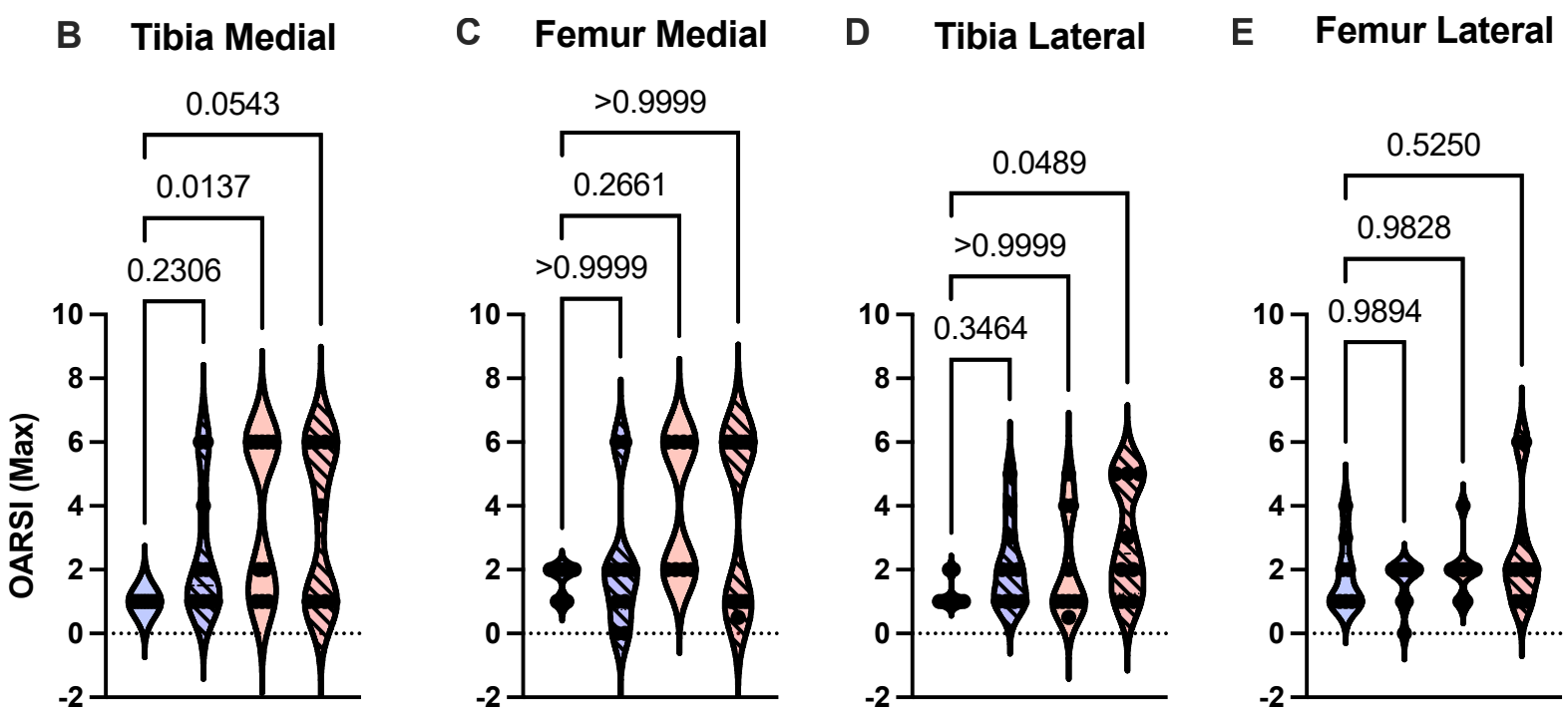
B Tibia Medial
C Femur Medial
D Tibia Lateral
E Femur Lateral
OARSI (Max)
0.0543
0.0137
0.2306
>0.9999
0.2661
>0.9999
0.0489
>0.9999
0.3464
0.5250
0.9828
0.9894
10
8
6
4
2
0
-2

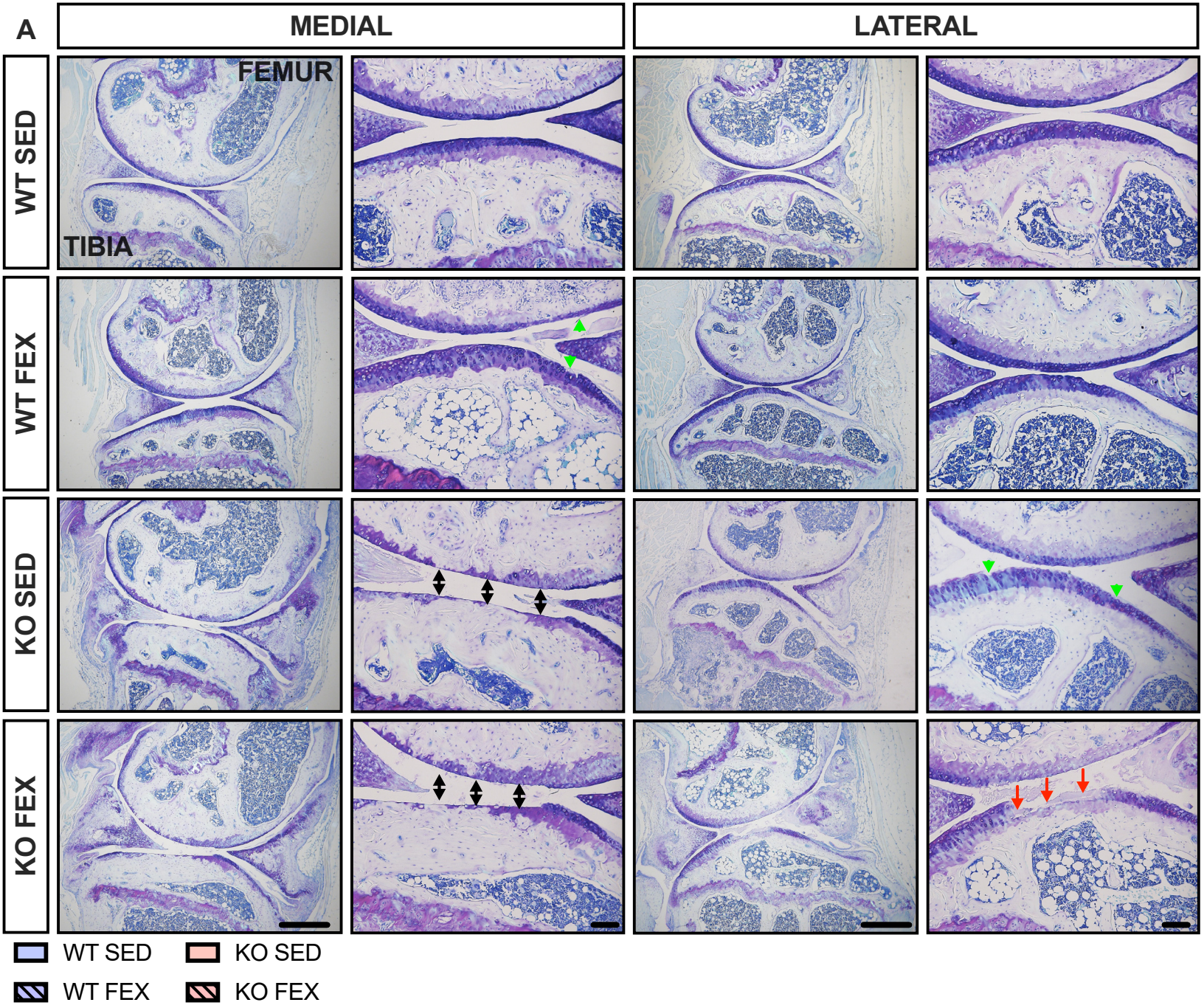
A
MEDIAL
LATERAL
WT SED
WT FEX
KO SED
KO FEX
FEMUR
TIBIA
WT SED
KO SED
WT FEX
KO FEX

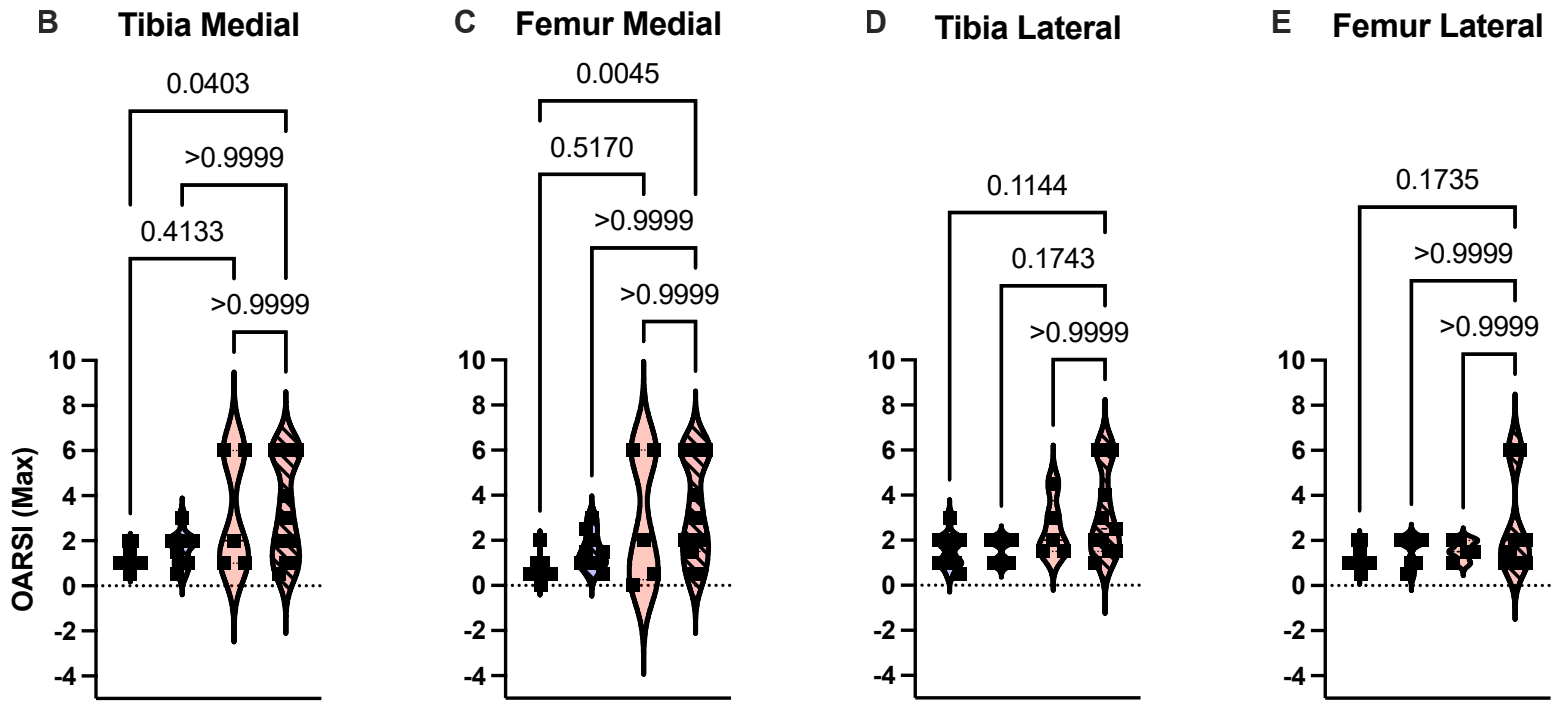
B
Tibia Medial
0.0403
>0.9999
0.4133
>0.9999
C
Femur Medial
0.0045
0.5170
>0.9999
>0.9999
D
Tibia Lateral
0.1144
0.1743
>0.9999
E
Femur Lateral
0.1735
>0.9999
>0.9999
OARSI (Max)
10
8
6
4
2
0
-2
-4

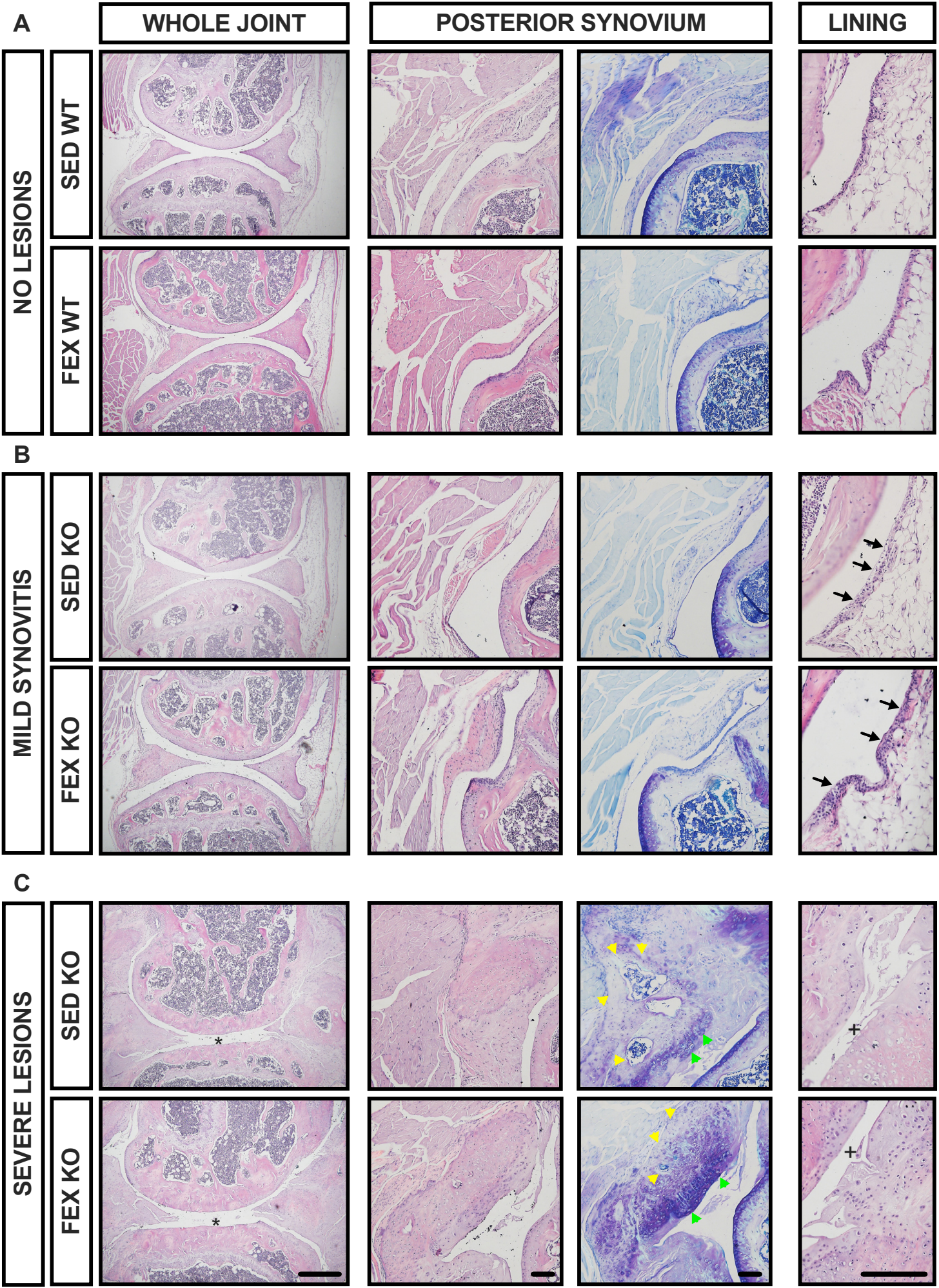
A
WHOLE JOINT
POSTERIOR SYNOVIUM
LINING
NO LESIONS
SED WT
FEX WT
B
MILD SYNOVITIS
SED KO
FEX KO
C
SEVERE LESIONS
SED KO
FEX KO

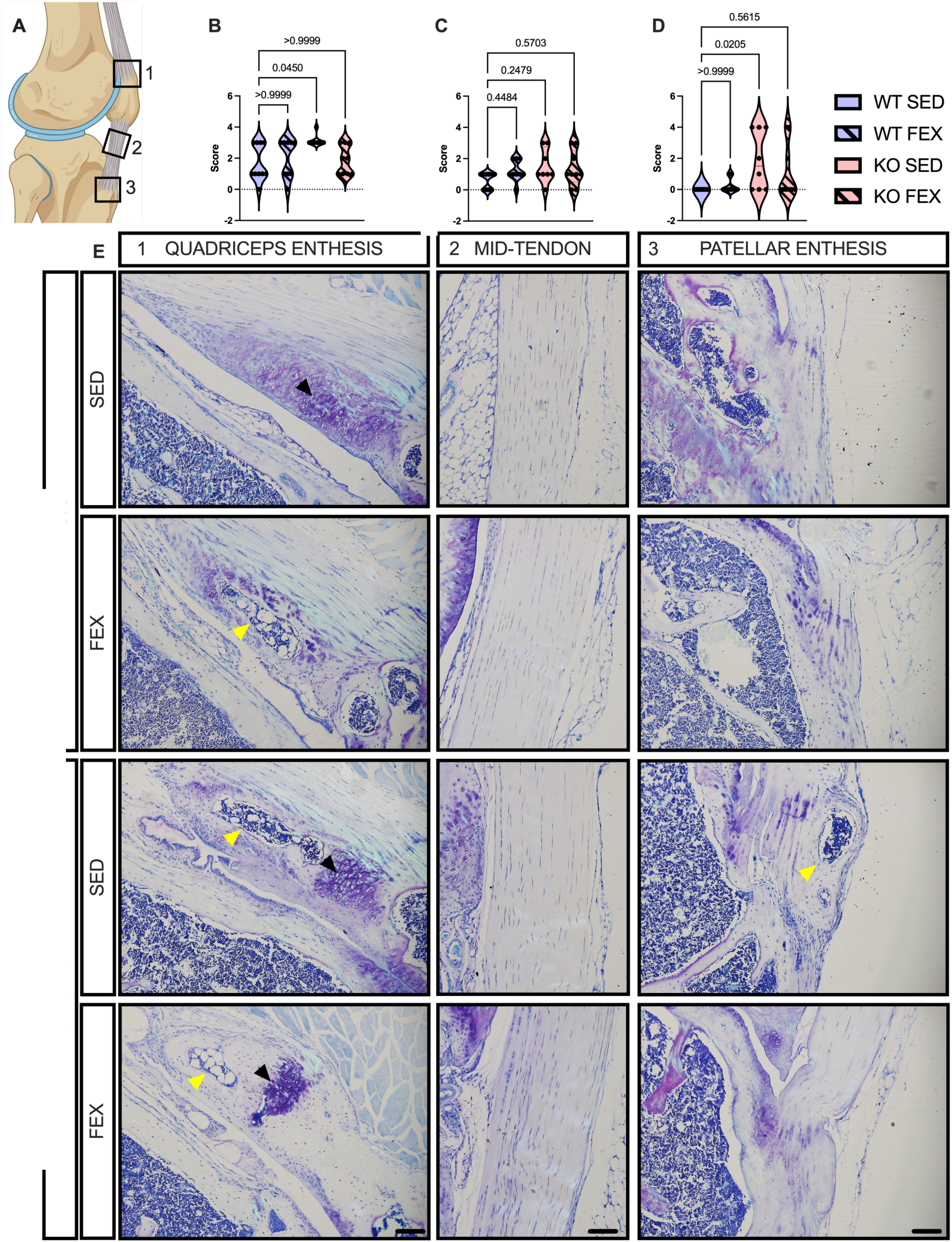
A
1
2
3
B
>0.9999
0.0450
>0.9999
Score
C
0.5703
0.2479
0.4484
Score
D
0.5615
0.0205
>0.9999
Score
WT SED
WT FEX
KO SED
KO FEX
E
1 QUADRICEPS ENTHESIS
2 MID-TENDON
3 PATELLAR ENTHESIS
SED
FEX
SED
FEX

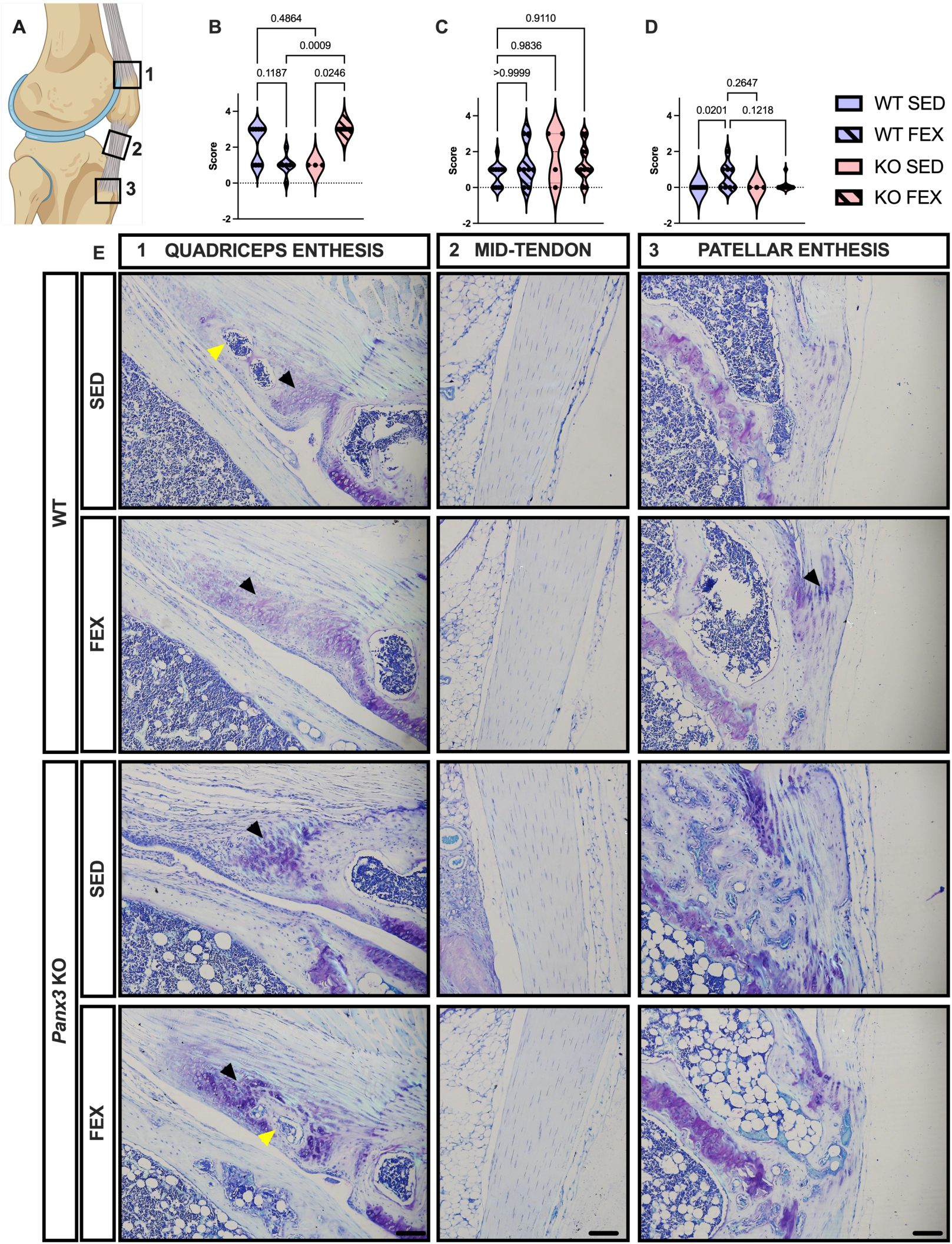
A
1
2
3
B
0.4864
0.0009
0.1187
0.0246
Score
C
0.9110
0.9836
>0.9999
Score
D
0.2647
0.0201
0.1218
Score
WT SED
WT FEX
KO SED
KO FEX
E
1 QUADRICEPS ENTHESIS
2 MID-TENDON
3 PATELLAR ENTHESIS
WT
SED
FEX
Panx3 KO
SED
FEX

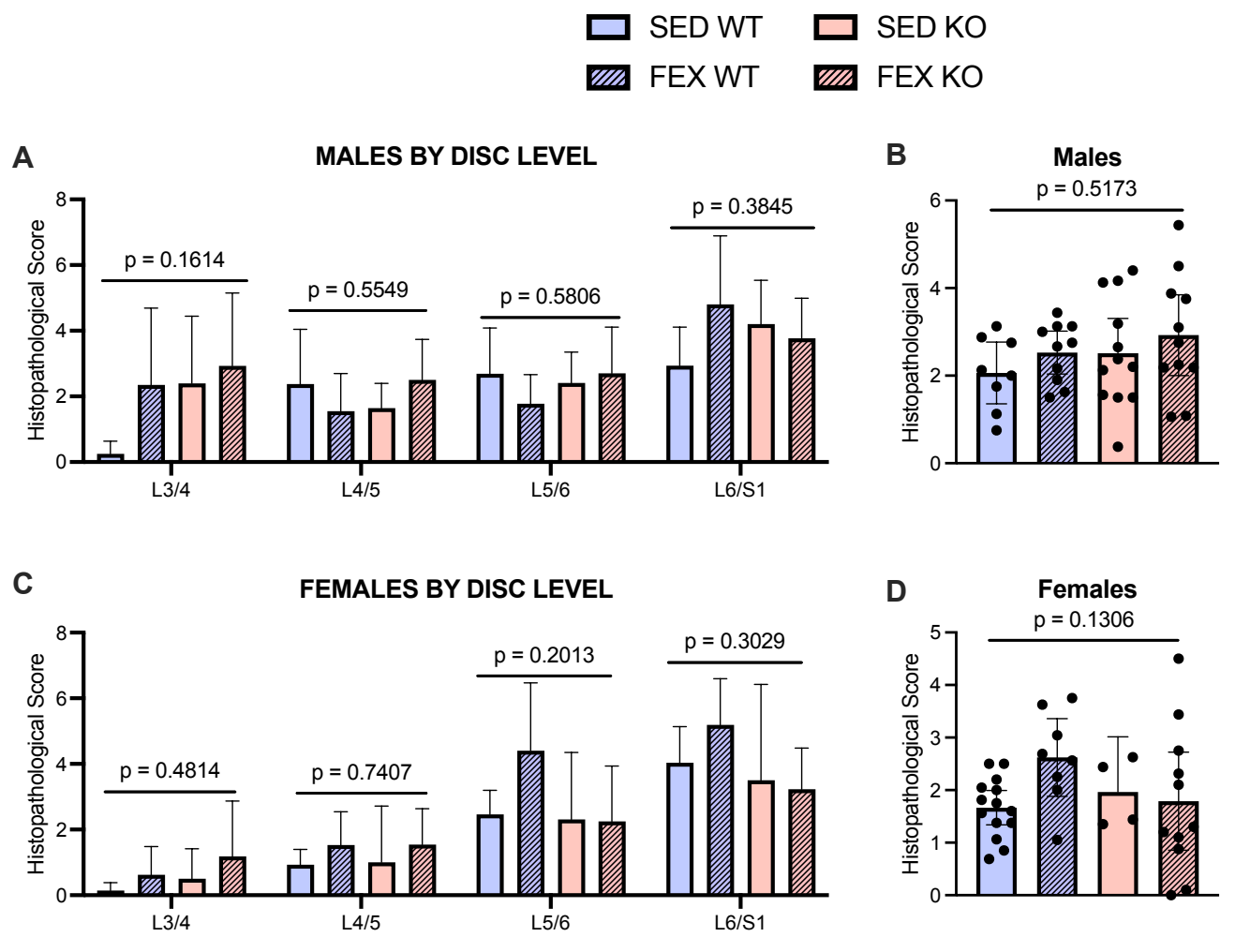
SED WT
SED KO
FEX WT
FEX KO
A
MALES BY DISC LEVEL
Histopathological Score
p = 0.1614
p = 0.5549
p = 0.5806
p = 0.3845
L3/4
L4/5
L5/6
L6/S1
B
Males
p = 0.5173
C
FEMALES BY DISC LEVEL
p = 0.4814
p = 0.7407
p = 0.2013
p = 0.3029
D
Females
p = 0.1306